

Nonlinear susceptibility: Evidence for antiferroquadrupolar fluctuations and a nonmagnetic Γ_1 ground state in the heavy fermion superconductor $\text{PrOs}_4\text{Sb}_{12}$

E. D. Bauer,* P.-C. Ho, and M. B. Maple

Department of Physics and Institute for Pure and Applied Physical Sciences, University of California, San Diego, La Jolla, California 92093, USA

T. Schauerte and D. L. Cox

Department of Physics, University of California, Davis, California 95616, USA

F. B. Anders

Institut für Festkörperphysik, Technical University Darmstadt, 64289 Darmstadt, Germany

(Received 23 August 2005; published 23 March 2006)

Nonlinear susceptibility (χ_3) measurements were performed on single crystals of the heavy fermion superconductor $\text{PrOs}_4\text{Sb}_{12}$ in order to probe the nature of the Pr^{3+} ground state in the crystalline electric field. Calculations of $\chi_3(T)$ have been carried out (i) within a mean field model of intersite magnetic and quadrupolar interactions for an ionic (zero hybridization) crystal field Γ_1 singlet ground state and a first excited state magnetic triplet, and (ii) within a two-channel Anderson impurity model assuming a Γ_{23} doublet ground state. The experimental χ_3 results are in best agreement with the nonmagnetic Γ_1 ground state in the tetrahedral crystalline electric field of the Pr^{3+} ions with antiferroquadrupolar intersite coupling and weak antiferromagnetic intersite coupling.

DOI: [10.1103/PhysRevB.73.094511](https://doi.org/10.1103/PhysRevB.73.094511)

PACS number(s): 74.70.Tx, 65.40.-b, 71.27.+a, 75.30.Mb

I. INTRODUCTION

Intermetallic compounds containing praseodymium provide a wealth of opportunities with which to investigate quadrupolar interactions in strongly correlated electron systems. In cubic materials, the crystalline electric field (CEF) splits the $J=4$ multiplet of Pr^{3+} into orbitally degenerate states that carry quadrupole moments, i.e., anisotropic charge distributions.¹ The interaction between these quadrupole moments and the conduction electrons or between the quadrupole moments themselves can give rise to strongly correlated electron phenomena such as heavy fermion behavior, quadrupolar ordering, and quantum criticality, in a manner analogous to the interactions of the magnetic moments of many Ce-, Yb-, or U-based materials. Examples of strong quadrupolar interactions are found in the filled skutterudite compounds that have the chemical formula RT_4X_{12} (R =alkali metal, alkaline earth, rare earth, or actinide; T =Fe, Ru, Os; X =P, As, Sb).²⁻⁴ For instance, the compound $\text{PrFe}_4\text{P}_{12}$ undergoes a transition to an ordered state below 6 K that was originally attributed to antiferromagnetic (AFM) order,⁵ but later identified with antiferroquadrupolar (AFQ) order.⁶ The compound $\text{PrFe}_4\text{P}_{12}$ exhibits quantum criticality associated with the suppression of the AFQ state in magnetic fields,⁷ resulting in the formation of a heavy Fermi liquid state above the quadrupolar quantum critical point (QCP).⁸ In contrast, the compound $\text{PrFe}_4\text{Sb}_{12}$ is a heavy fermion magnet,^{9,10} with a crossover to non-Fermi liquid behavior in magnetic fields above $H=3$ T.⁹ The compound $\text{PrOs}_4\text{Sb}_{12}$ is a heavy fermion superconductor with a transition temperature $T_c=1.85$ K,^{11,12} which undergoes a transition to an ordered state in high magnetic fields¹² that has been attributed to antiferroquadrupolar order,¹³ suggesting

that the extraordinary normal and superconducting properties of this compound may be associated with its proximity to a field-induced quadrupolar QCP, in accord with a previous conjecture.¹⁴ The superconducting properties of $\text{PrOs}_4\text{Sb}_{12}$ (Refs. 11 and 15–17) are unusual and quite different from those of other heavy fermion superconductors; this has prompted speculation that the unconventional superconductivity may be mediated by quadrupolar fluctuations,^{12,18–21} instead of the magnetic spin fluctuations believed to mediate Cooper pairing in the Ce- and U-based heavy fermion superconductors. A double superconducting transition at $T_{c1}=1.85$ K and $T_{c2}=1.75$ K, observed in a variety of measurements, e.g., specific heat,^{12,22,23} magnetization,^{24,25} thermal expansion,²⁶ and penetration depth^{27,28} suggest a multi-component order parameter.^{29,30} Evidence for a third superconducting transition at ≈ 0.6 K has been obtained from a kink in the lower critical field $H_{c1}(T)$ and the critical current $I_c(T)$.¹⁶ Multiple superconducting phases with distinct point-node gap structures have also been proposed, based upon angular-dependent thermal conductivity measurements in magnetic fields.³¹ Penetration depth measurements reveal that $\lambda(T)$ has a T^2 dependence between ≈ 0.1 and 0.6 K, which has been taken as evidence for point nodes in the gap function and found to be consistent with calculations based on triplet superconductivity.³² However, the activated behavior of the magnetic penetration depth determined from muon-spin-relaxation (μSR) experiments³³ and the nuclear spin-lattice relaxation $1/T_1$ (Ref. 34) indicate an isotropic superconducting gap. Furthermore, zero-field μSR measurements on $\text{PrOs}_4\text{Sb}_{12}$ reveal a time-reversal-symmetry-breaking state below T_c ,³⁵ which suggests a rather original superconducting state.

While the CEF ground state has been (more or less) established in $\text{PrOs}_4\text{Sb}_{12}$, the nature of the quadrupolar fluctua-

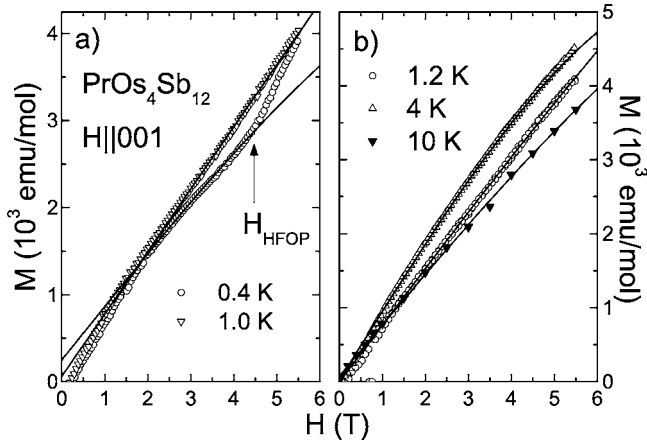


FIG. 1. Magnetization M vs magnetic field H of $\text{PrOs}_4\text{Sb}_{12}$ (a) below 1 K and (b) above 1 K with $H \parallel [001]$. The solid lines are fits of Eq. (1) to the $M(H)$ data.

tion in this material is less clear. A cubic CEF will split the $\text{Pr}^{3+} J=4$ multiplet into a nonmagnetic Γ_1 singlet, a nonmagnetic Γ_3 doublet, and two magnetic triplets (Γ_4 and Γ_5) (in O_h symmetry).¹ The slightly reduced T_h symmetry appropriate for the filled skutterudite structure causes an additional mixing of the magnetic triplets (now labeled $\Gamma_4^{(1)}$ and $\Gamma_4^{(2)}$).³⁶ Recent inelastic neutron scattering measurements, consistent with previous experiments,^{12,37} reveal a CEF energy-level scheme (in T_h symmetry): Γ_1 ground state and a low-lying $\Gamma_4^{(2)}$ first excited state separated by $\delta \sim 7.8$ K, followed by $\Gamma_4^{(1)}$ (135 K) and Γ_{23} (205 K) excited states.³⁸ Neutron diffraction measurements indicate the presence of a small antiferromagnetic moment ($\mu_{AFM} = 0.025 \mu_B$) parallel to the $[010]$ direction in magnetic fields above $H \sim 5$ T at $T = 0.25$ K.¹³ A crystalline electric field analysis based on a Γ_1 ground state suggests that antiferroquadrupolar order arises from a level crossing of the Γ_1 ground state with an excited state in magnetic fields.^{39,40} This crossing of the CEF levels is believed to give rise to the high-field-ordered phase (HFOP) in high magnetic fields ($H > 4$ T) below 2 K.^{12,15,24,25} The power law T dependence of the electrical resistivity¹² near the HFOP suggests proximity to an antiferroquadrupolar quantum critical point. It has been proposed that such quadrupolar fluctuations lead to the softening of the elastic $(C_{11} - C_{12})/2$ and C_{44} modes.⁴¹

Measurements of the nonlinear susceptibility χ_3 , the third-order coefficient in the magnetic field development of the magnetization, constitute a useful technique for obtaining information about quadrupolar interactions that was applied to rare-earth intermetallic compounds by Morin and Schmitt.⁴² In addition, in the ionic limit (weak hybridization of f orbitals to other states), this technique can distinguish between a magnetic ground state (in which χ_3 is isotropic, large, and negative with a T^{-3} temperature dependence, as can be seen by an expansion of the Brillouin function), and a non-Kramers Γ_3 doublet, in which χ_3 is anisotropic and exhibits a positive T^{-1} divergence as $T \rightarrow 0$ K when the magnetic field is applied along one of the principal axes; i.e., $H \parallel [100]$. Nonlinear susceptibility χ_3 measurements can also reveal a nonmagnetic Γ_1 singlet, which will produce nearly isotropic

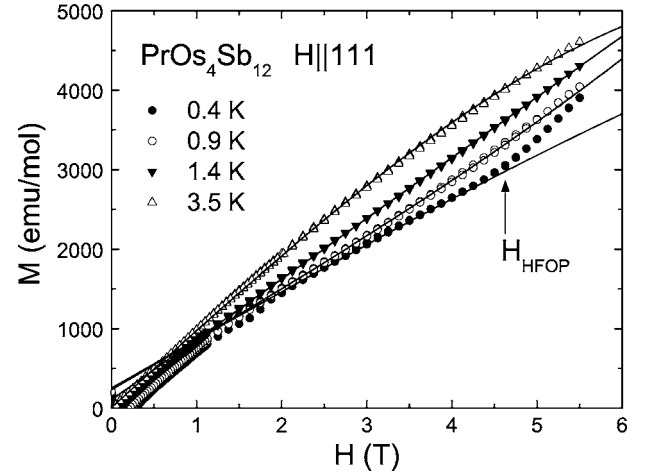


FIG. 2. M vs H of $\text{PrOs}_4\text{Sb}_{12}$ for $0.4 \text{ K} \leq T \leq 4.5 \text{ K}$ with $H \parallel [111]$. The solid lines are fits of Eq. (1) to the $M(H)$ data.

and nondivergent nonlinear susceptibility. In this paper, we present measurements of the nonlinear susceptibility of $\text{PrOs}_4\text{Sb}_{12}$ in order to probe both the nature of the ground state and the quadrupolar fluctuations in this material, and find that our data favor a nonmagnetic Γ_1 crystal field ground state with induced moment antiferroquadrupolar and antiferromagnetic interactions between Pr ions; a nonmagnetic doublet ground state treated within an Anderson impurity model produces unsatisfactory agreement with the data.

II. EXPERIMENTAL DETAILS

Single crystals of $\text{PrOs}_4\text{Sb}_{12}$ were grown in an Sb flux.² Magnetization measurements were performed in a commercial superconducting quantum interference device magnetometer at temperatures between 1.8 and 20 K in magnetic fields up to $H = 5.5$ T. The background signal of the sample holder was found to be 1–5 % of the total signal, within the standard deviation of the measurement, and was, therefore, neglected in the subsequent analysis. Magnetization measurements down to $T = 0.35$ K up to $H = 5.5$ T were performed in a ^3He Faraday magnetometer. In this case, the background magnetization was subtracted from the data. In general, differences between the two experiments with the same field and temperature conditions were less than 10%.

Our original magnetic susceptibility $\chi_1(T)$ data (Ref. 11), used here to determine model parameters, were obtained from a collection of single crystals grown from an antimony rich flux. In consequence, a substantial diamagnetic signal from surface antimony inclusions is likely present. To correct for this, we matched the maximum in our data to the maximum in the data from a large single crystal of Ref. 24 and adjusted the estimated fraction of antimony contribution accordingly; this corresponds to a 15% weight fraction of antimony.

III. RESULTS

Figures 1 and 2 show representative magnetization $M(H)$ curves for $H \parallel [001]$ and $H \parallel [111]$, respectively. The data do

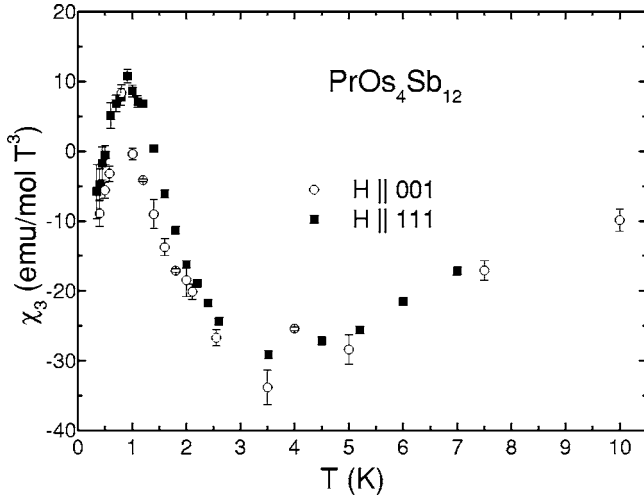


FIG. 3. Nonlinear susceptibility $\chi_3(T)$ of $\text{PrOs}_4\text{Sb}_{12}$ with $H \parallel [001]$ (circles) and $H \parallel [111]$ (squares).

not scale as some function of H/T as expected for a magnetic (Γ_5) ground state. Above 2 K, the $M(H)$ curves have negative curvature and appear to exhibit positive curvature at temperatures close to 1 K; an upturn in the magnetization appears at a magnetic field $H_{HFOP} \sim 4.5$ T below 1 K, indicating the presence of a high-field-ordered phase found in previous measurements.^{12,15,24,25} In the paramagnetic state, the third-order susceptibility χ_3 is a measure of the leading nonlinearity of the magnetization

$$M = M_0 + \chi_1 H + \frac{\chi_3}{3!} H^3 \dots \quad (1)$$

in the direction of the applied magnetic field \vec{H} , where M_0 takes into account extrinsic effects, e.g., trapped flux in the superconducting magnet, and χ_1 is the usual magnetic susceptibility. The nonlinear susceptibility χ_3 was obtained from fits of the $M(H)$ data to Eq. (1) and is shown in Fig. 3.

For temperatures above 1 K [Fig. 1(b)], fits of Eq. (1) to the $M(H)$ data for $1 \text{ T} \leq H \leq 5.5 \text{ T}$ were performed to obtain χ_3 ; whereas below 1 K [Fig. 1(a)], the fits to the data were carried out for magnetic fields less than $H_{HFOP} \sim 4$ T and in the normal state [$H_{c2}(T) \sim 1.5\text{--}2.2$ T (Ref. 11)]. It is possible that these fits below 1 K somewhat overestimate the nonlinear contribution due to the limited fit range. The magnetic susceptibility $\chi_1(T)$ determined from these fits agrees well with bulk measurements.^{15,24} Fits of the $M(H)$ data for $H \parallel [111]$ over comparable field ranges (Fig. 2) yield similar results.

Shown in Fig. 3 is the nonlinear susceptibility χ_3 vs T for $H \parallel [001]$ and $H \parallel [111]$. With decreasing temperature, χ_3 is negative and reaches a minimum at ~ 4 K, followed by a positive maximum at ~ 1 K, before diverging negatively below 1 K for both field directions. The nonlinear susceptibility is nearly isotropic (although χ_3 for $H \parallel [001]$ may be smaller in magnitude than for $H \parallel [111]$); the T dependence and magnitude are in excellent agreement with the measurements of Tenya *et al.*⁴³

IV. ANALYSIS

A. Γ_1 ground state calculations

We have modeled the nonlinear susceptibility in the Γ_1 singlet ground state model using the molecular field formalism of Morin and Schmitt⁴² augmented by the additional crystal field term appropriate to the tetrahedral symmetry noted elsewhere.³⁶ We have carried this out in the ionic limit (zero hybridization) of the Anderson model. The tetrahedral symmetry turns out to be critical to assure a reasonable concomitant description of the linear and nonlinear susceptibility; in the cubic field, it is impossible to get comparable negative and positive lobes for the nonlinear susceptibility as we have found here.

We have defined the allowed sixth-order T terms in the crystal field as

$$\mathcal{H}_{tet} = Y \left[(J_x^2 J_y^2 J_x^2 + J_y^2 J_z^2 J_y^2 + J_z^2 J_x^2 J_z^2) - \frac{1}{2} (J_x^4 J_y^2 + J_y^4 J_x^2 + J_y^2 J_z^4 + J_z^4 J_y^2 + J_z^2 J_x^4 + J_x^4 J_z^2) \right] \quad (2)$$

with J_i ($i=x, y, z$) angular momentum operators in the $J=4$ ground multiplet. The crystal field Hamiltonian is then determined from the usual Lea-Leask-Wolf¹ cubic terms parametrized by W, x and the above term. We set the crystal field parameters by matching to the level scheme determined from neutron scattering³⁸; specifically, we placed the Γ_{23} doublet at 205 K (this determines W for a given x) and set Y for the tetrahedral term by setting the first excited triplet at 7.7 K in agreement with Ref. 38. The best simultaneous description of linear and nonlinear susceptibilities is then obtained for $x=0.465$, $W=3.112$ K, and $Y=0.166$ K. We note that the relation between our Y parameter and y of Refs. 36 and 38 is $y=1.86Y/W$. For these parameters, we find the second excited crystal field triplet $\Gamma_4^{(2)}$ at 134 K in good agreement with neutron scattering data.^{12,37,38}

To obtain our estimates of χ_1 and χ_3 , we compute noninteracting susceptibilities by numerically adding small magnetic fields h and normalized stresses η_i ($i=[100], [111]$) to the crystal field Hamiltonian, computing the free energy F^0 from the ionic partition function Z^0 in the small applied fields, and estimating the derivatives with respect to the applied fields via suitable and standard numerical multipoint formulas. Note that the stresses are uniaxial along principal axes or body diagonals of the relevant tetrahedron. The stresses η_i are measured in units of energy and linearly couple to the quadrupolar operators $[\sqrt{3}(J_x^2 - J_y^2), 2J_z^2 - J_x^2 - J_y^2]$ for $i=[100]$, and $(J_x J_y + J_y J_x, J_y J_z + J_z J_y, J_z J_x + J_x J_z)$ for $i=[111]$.

The relevant noninteracting susceptibilities are

$$\chi_1^0(T) = - \left. \frac{\partial^2 F^0(T, \vec{h}, \vec{\eta}_i)}{\partial h_z^2} \right|_{\vec{h}, \vec{\eta}_i=0}, \quad (3)$$

$$\chi_{qi}^0(T) = - \left. \frac{\partial^2 F^0(T, h, \eta_i)}{\partial \eta_i^2} \right|_{h, \eta_i=0}, \quad (4)$$

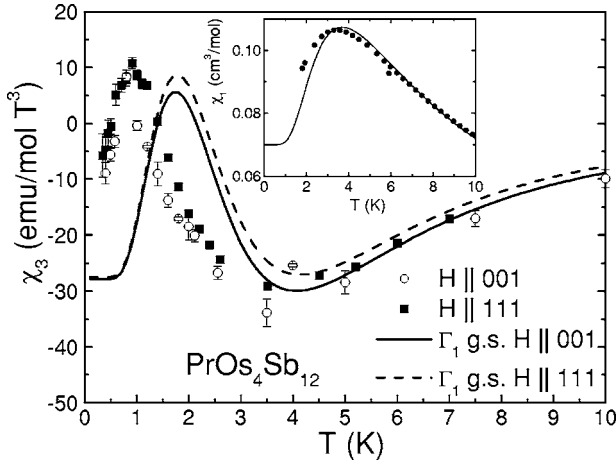


FIG. 4. $\chi_3(T)$ of $\text{PrOs}_4\text{Sb}_{12}$ with $H \parallel [001]$ (circles) and $H \parallel [111]$ (squares), along with the Γ_1 ground state calculations as discussed in the text for $H \parallel [001]$ (solid line) and $H \parallel [111]$ (dashed line). Inset: Magnetic susceptibility $\chi_1(T)$ along with the Γ_1 ground state calculations as discussed in Sec. IV A (solid line).

$$\chi_{qmi}^0(T) = -2 \left. \frac{\partial^3 F^0(T, h, \eta_i)}{\partial \eta_i \partial h^2} \right|_{h, \eta_i=0}, \quad (5)$$

$$\chi_{3i}^0(T) = -6 \left. \frac{\partial^4 F^0(T, \vec{h}, \eta_i)}{\partial h_i^4} \right|_{h, \eta_i=0}, \quad (6)$$

which are, respectively, the linear magnetic susceptibility, linear quadrupolar susceptibility, parastriction susceptibility, and nonlinear magnetic susceptibility. In the latter case, we differentiate with respect to fields along the z -axis ([100]) or [111] directions.

Next, we introduce intersite Curie-Weiss interaction parameters n for magnetic susceptibility, and g_i for the quadrupolar susceptibilities, in terms of which the molecular field theory of the linear and nonlinear susceptibilities gives⁴²

$$\chi_1(T) = \frac{\chi_1^0(T)}{1 - n\chi_1^0(T)} \quad (7)$$

$$\chi_{3i}(T) = \frac{\chi_{3i}^0(T)}{[1 - n\chi_1^0(T)]^4} + 2g_i \frac{[\chi_{qmi}^0(T)]^2}{[1 - n\chi_1^0(T)]^4 [1 - g_i\chi_{qi}^0(T)]}. \quad (8)$$

Note that while the Pr site has tetrahedral symmetry, the overall crystal symmetry is cubic and thus has two independent χ_3 components.

We find that the measured linear susceptibility is slightly suppressed with respect to the noninteracting ionic limit, requiring a weakly antiferromagnetic Curie-Weiss constant $n = -0.12$ mol/emu [$|n\chi_1^0(T_{1,max})| = 0.012$, where $T_{1,max}$ is the temperature at which the ionic linear susceptibility peaks]. This is shown in the inset to Fig. 4. We note that with this weak antiferromagnetic coupling and no intersite quadrupolar interactions, the nonlinear susceptibility given by the above equations shows a similar shape to the data but the main negative lobe magnitude is too small by approximately

20% (about 6 emu/mol T³). We further note that the two lobe characters of the experimental nonlinear susceptibility require crystal field parameters in this vicinity, and that to fit the magnitude of χ_3 requires any antiferromagnetic coupling to be small, since the fourth power Curie-Weiss factor rapidly suppresses the magnitude of χ_3 if n is raised too far in magnitude.

The term in χ_3 due to quadrupolar interactions is negative definite for antiferroquadrupolar coupling and a Γ_1 ground state, and positive definite for subcritical ferroquadrupolar coupling. Hence, we are guided to fit the data in the parameter region with antiferroquadrupolar intersite interactions. It can be seen from the above equations that the quadrupolar contribution to χ_3 saturates for infinite antiferroquadrupolar coupling to the form

$$\chi_{3,q\infty}(T) = -2 \frac{[\chi_{qmi}^0(T)]^2}{[1 - n\chi_1^0(T)]^4 \chi_{qi}^0(T)}. \quad (9)$$

For our crystal field parameters, and the weak antiferromagnetic coupling, $\chi_{3,q\infty}$ has minima at 3.2 K (4 K) for $H \parallel [100]$ ($H \parallel [111]$) of -14 emu/mol T³ (-12 emu/mol T³). The leading term in χ_3 [first term on the right-hand side of Eq. (8)], which is of purely magnetic origin, already contributes approximately -25 emu/mol T³ to χ_3 . To get the requisite downward correction of about -5 emu/mol T³ from the quadrupolar term requires contributions at about half of the minimum values of $\chi_{3,q\infty}$. This implies nearly critical antiferroquadrupolar coupling.

As shown in Fig. 4, we find that to fit the nonlinear susceptibility best and maintain near isotropy for the [100] and [111] directions requires strongly antiferroquadrupolar couplings g_i , with $g_{100} = -0.158$ K ($|g_{100}\chi_{q100}^0(T_{100,max})| = 0.95$, where the ionic linear [100] quadrupolar susceptibility peaks at $T_{100,max}$), and $g_{111} = -0.349$ K ($|g_{111}\chi_{q111}^0(T_{111,max})| = 0.95$, where $T_{111,max}$ is the temperature at which the linear [111] susceptibility peaks). Hence, this analysis suggests that $\text{PrOs}_4\text{Sb}_{12}$ is in close proximity to antiferroquadrupolar transitions for both field directions. This is consistent with the observed field-induced ordering and with the zone boundary softening of magnetic excitations.⁴⁴

The heavy fermion behavior observed in this material is not directly accounted for by the ionic model in that some linear specific heat remains after accounting for the Schottky anomaly of the excited triplet level. Of course, the Schottky peak will be broadened in the real material by at least two effects: (i) in the ionic model, intersite coupling will induce dispersion which will yield a minimum excitation energy at a zone center of about 2.6 K; (ii) hybridization will induce damping and a finite width to the singlet-triplet excitations. Both mechanisms will enhance the low temperature specific heat above the ionic Schottky anomaly, and the broadening will lift the exponential suppression approach of the linear susceptibility to its low temperature value, which appears consistent with experiment as well.

B. Γ_{23} ground state calculations

For completeness, and since earlier work supposed the possibility of a nonmagnetic ground doublet, we also exam-

ine the nonlinear susceptibility arising from a non-Kramers Γ_{23} doublet.

In order to describe the gross features of the experimentally measured $\chi_1(T)$ and $\chi_3(T)$ data assuming a Γ_{23} ground state, we study the two-channel Anderson impurity model⁴⁵ in the tetrahedral system but in the cubic limit, taking into account the Γ_{23} quadrupolar doublet ground state in the $J=4$ ($4f^2$) configuration of the Pr^{3+} ion, as well as all excited crystal field states in the $4f^2$ configuration, i.e., the $\Gamma_4^{(1),(2)}$ triplet states and a Γ_1 singlet. For simplicity, we restrict ourselves to the magnetic Γ_6 doublet (with energy 1.9 eV) in the $J=\frac{9}{2}$ ($4f^3$) configuration. We anticipate the qualitative low temperature behavior to be the same with the inclusion of all f^2 and f^3 excited states. Only valence fluctuations between $4f^2$ and $4f^3$ are considered. In our model, the localized Pr ion hybridizes via a spherical matrix element V with conduction electrons carrying both spin ($\sigma=\uparrow, \downarrow$) and quadrupolar ($\mu=+, -$) quantum labels. The corresponding Hamiltonian is given by

$$H = \sum_{k\sigma\mu} \epsilon_{k\sigma\mu} c_{k\sigma\mu}^\dagger c_{k\sigma\mu} \sum_{\sigma} E_{\sigma} |\sigma\rangle\langle\sigma| + \sum_M E_M |M\rangle\langle M| \\ + V \sum_{k\sigma\mu M} (C_{\sigma\mu;M} c_{k\sigma\mu}^\dagger |\sigma\rangle\langle M| + \text{H. c.}),$$

where the Pr^{2+} state $|\sigma\rangle$ represents the magnetic Kramers doublet with energy E_{σ} and $|M\rangle$ represents the Γ_{23} , $\Gamma_4^{(1)}$, $\Gamma_4^{(2)}$, and Γ_1 states of Pr^{3+} . The operator $c_{k\sigma\mu}^\dagger$ creates a conduction electron with wave number k , spin σ , channel index μ , and kinetic energy $\epsilon_{k\sigma\mu}$. In these calculations, the energies of the excited f -electron states $E_M=(E_{\Gamma_4^{(1)}}, E_{\Gamma_4^{(2)}}, E_{\Gamma_6}, E_{\Gamma_1})$ and E_{σ} are measured from that of the ground state ($E_{\Gamma_{23}}$). The Clebsch-Gordan coefficient $C_{\sigma\mu;M}$ is given by $\langle\sigma|f_{\sigma\mu}|M\rangle$, where $f_{\sigma\mu}$ annihilates an f electron. The linear and nonlinear susceptibilities are evaluated in the framework of the non-crossing approximation,^{46,47} which is the lowest order self-consistent expansion in the hybridization V . This approximation is known to describe the physics of the two-channel Anderson model correctly.⁴⁸

The calculated $\chi_3(T)$ (with $H||[001]$ and $[111]$) is displayed in Fig. 5, using values of $T_K=0.21$ K, $V=0.4$ eV, and a CEF level scheme $\Gamma_4^{(2)}$ (10 K), $\Gamma_4^{(1)}$ (160 K), and E_{Γ_1} (370 K), consistent with previous results.^{12,37,38} With this choice of parameters, we are in the Kondo regime of the model with an f^2 occupancy of 0.97 at low temperatures. χ_3 along $[011]$ is straightforwardly interpolated between $[001]$ and $[111]$, i.e., $\chi_3^{011} = (1/4)\chi_3^{001} + (3/4)\chi_3^{111}$.

The negative divergence of χ_3 develops in all directions theoretically and robustly arises from (i) divergent contributions from the excited f^3 magnetic states noted previously⁴⁶ [these go as $-\ln^2(T)/T$], and (ii) divergent contributions arising from “disconnected” diagrams which vary as $-1/T$ and are proportional to the quantum weight of $\Gamma_4^{(2)}$ states. Both contributions are suppressed in the zero hybridization ionic limit of Ref. 42 by vanishingly small Boltzmann weights. The model calculations give a positive maximum in χ_3 for the $[111]$ direction, which corresponds to a sampling of the

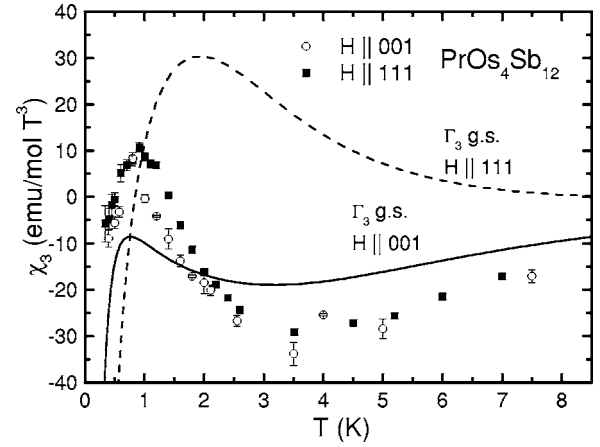


FIG. 5. $\chi_3(T)$ of $\text{PrOs}_4\text{Sb}_{12}$ with $H||[001]$ (circles) and $H||[111]$ (squares) along with the Anderson impurity calculations with the Γ_{23} ground state as discussed in Sec. IV B for $H||[001]$ (solid line) and $H||[111]$ (dashed line).

ferroquadrupolar response of the (xy, xz, yz) symmetry quadrupolar moment of the $\Gamma_4^{(2)}$ triplet; such a relative positive value of the $[111]$ limit to the $[100]$ limit is found in the ionic limit for a $\Gamma_4^{(2)}$ ground state in cubic symmetry, and the finite quantum weight of the $\Gamma_4^{(2)}$ here leads to the intermediate temperature maximum.

We note that this theoretical treatment of χ_3 is not in good agreement with the experimental $\chi_3(T)$ curves (Fig. 3); in particular, the relatively large anisotropy between the $[100]$ and $[111]$ directions is not observed in the nearly isotropic experimental χ_3 data. However, on the basis of the anisotropy, these calculations may be useful in distinguishing between the two possible nonmagnetic ground states of Pr (or U) in cubic symmetry. Furthermore, the theory may provide a more realistic description of the behavior of these materials containing Pr or U with the following improvements: (i) the model excludes excited f^3 states, and as such, cannot properly estimate the quantum weight of the $\Gamma_4^{(2)}$ state (an overestimate will overemphasize the positive contribution associated with the $\Gamma_4^{(2)}$ symmetry quadrupolar moment) and (ii) ignores intersite interactions. These can provide induced moment antiferromagnetic correlations between $\Gamma_4^{(2)}$ magnetic moments that can (i) reduce $\chi_1(0)$ relative to the peak value, which may account for the disagreement between theory and experiment in $\chi_1(T)$, and (ii) induce $\Gamma_4^{(2)}$ symmetry antiferroquadrupolar correlations (for the bcc symmetry of the skutterudites) which, in turn, would reduce the above-mentioned positive contributions to χ_3 along the $[111]$ direction. (Of course, these can be suppressed by direct, noninduced antiferroquadrupolar correlations of the $\Gamma_4^{(2)}$ states.)

V. CONCLUSIONS

In summary, nonlinear susceptibility measurements were performed on the heavy fermion superconductor $\text{PrOs}_4\text{Sb}_{12}$ to investigate the ground state properties. Calculations of χ_3 have been carried out within (i) an interaction ionic limit for a nonmagnetic singlet ground state, and (ii) a two-channel

Anderson impurity model assuming a quadrupolar Γ_{23} ground state. The experimental results, however, are in better agreement with ionic calculations including antiferroquadrupolar interactions within a nonmagnetic Γ_1 ground state, suggesting proximity to a quadrupolar quantum critical point in $\text{PrOs}_4\text{Sb}_{12}$, in accord with an earlier conjecture.¹⁴

Clearly, the analysis of χ_3 supports the notion that $\text{PrOs}_4\text{Sb}_{12}$ is close to an antiferroquadrupolar quantum critical point. This is bolstered empirically by evidence of antiferroquadrupolar order in applied magnetic field,^{15,17,24,25} and zone boundary softening of singlet-triplet excitations in the paramagnetic phase.⁴⁴ Hence, our analysis provides further support for the notion that antiferroquadrupolar fluctuations mediate superconductivity in this material, and this naturally can lead to multiple component order parameters in agreement with experimental findings.^{12,15,16,23,31}

What is perhaps most surprising is that $\text{PrOs}_4\text{Sb}_{12}$ could sustain negligible antiferromagnetic couplings based upon our analysis of the linear and nonlinear susceptibility while having large intersite antiferroquadrupolar couplings. If the

interactions are dominated by either conduction electron mediated Coulombic multipole exchange or hybridization driven exchange, one would anticipate more comparable magnitudes. At the same time, the relatively large distance between Pr ions in this structure certainly suggests that weak coupling is plausible. On the other hand, oscillatory strain mediated couplings between quadrupole moments are, of course, possible, and this may be the source of the discrepancy between magnetic and quadrupolar interactions and merits further examination in this fascinating material.

ACKNOWLEDGMENTS

Research at UCSD was supported by the U.S. DOE (Grant No. DE-FG02-04ER46105), the NSF (Grant No. DMR 03351733), and the NEDO International Joint Research Program. T.S. and D.L.C. acknowledge support from the U.S. DOE, Office of Basic Energy Sciences, and Division of Materials Research. T.S. also acknowledges financial support from Deutsche Forschungsgemeinschaft.

*Present address: Los Alamos National Laboratory, Los Alamos, NM 87545, USA.

¹K. R. Lea, M. J. K. Leask, and W. P. Wolf, *J. Phys. Chem. Solids* **23**, 1381 (1962).

²E. D. Bauer, A. Ślebarski, E. J. Freeman, C. Sirvent, and M. B. Maple, *J. Phys.: Condens. Matter* **13**, 4495 (2001), and references therein.

³M. B. Maple, E. D. Bauer, N. A. Frederick, P.-C. Ho, W. M. Yuhasz, and V. S. Zapf, *Physica B* **328**, 29 (2003).

⁴Y. Aoki, H. Sugawara, H. Hisatomo, and H. Sato, *J. Phys. Soc. Jpn.* **74**, 209 (2005).

⁵M. S. Torikachvili, J. W. Chen, Y. Dalichaouch, R. P. Guertin, M. W. McElfresh, C. Rossel, M. B. Maple, and G. P. Meisner, *Phys. Rev. B* **36**, 8660 (1987).

⁶L. Hao, K. Iwasa, M. Nakajima, D. Kawana, K. Kuwahara, M. Kohgi, H. Sugawara, T. D. Matsuda, Y. Aoki, and H. Sato, *Acta Phys. Pol. B* **34**, 1113 (2003).

⁷T. Sakakibara *et al.*, *Physica B* (to be published).

⁸Y. Aoki, T. Namiki, T. D. Matsuda, K. Abe, H. Sugawara, and H. Sato, *Phys. Rev. B* **65**, 064446 (2002).

⁹E. Bauer, S. Berger, A. Galatanu, C. Paul, M. D. Mea, H. Michor, G. Hilscher, A. Grytsiv, P. Rogl, D. Kaczorowski, P. Rogl, T. Hermannsdörfer, and P. Fisher, *Physica B* **312-313**, 840 (2002).

¹⁰N. P. Butch, W. M. Yuhasz, P.-C. Ho, J. R. Jeffries, N. A. Frederick, T. A. Sayles, X. G. Zheng, M. B. Maple, J. B. Betts, A. H. Lacerda, F. M. Woodward, J. W. Lynn, P. Rogl, and G. Giester, *Phys. Rev. B* **71**, 214417 (2005).

¹¹E. D. Bauer, N. A. Frederick, P.-C. Ho, V. S. Zapf, and M. B. Maple, *Phys. Rev. B* **65**, 100506(R) (2002).

¹²M. B. Maple, P.-C. Ho, V. S. Zapf, N. A. Frederick, E. D. Bauer, W. M. Yuhasz, F. M. Woodward, and J. W. Lynn, *J. Phys. Soc. Jpn.* **71**, 23 (2002).

¹³M. Kohgi, K. Isawa, M. Nakajima, N. Metoki, A. Araki, N. Bernhoeft, J.-M. Mignot, A. Gukasov, H. Sato, Y. Aoki, and H. Sugawara, *J. Phys. Soc. Jpn.* **72**, 1002 (2003).

¹⁴M. B. Maple, E. D. Bauer, V. S. Zapf, E. J. Freeman, and N. A. Frederick, *Acta Phys. Pol. B* **32**, 3291 (2001).

¹⁵M. B. Maple, P.-C. Ho, N. A. Frederick, V. S. Zapf, W. M. Yuhasz, and E. D. Bauer, *Acta Phys. Pol. B* **34**, 919 (2003).

¹⁶T. Cichorek, A. C. Mota, F. Steglich, N. A. Frederick, W. M. Yuhasz, and M. B. Maple, *Phys. Rev. Lett.* **94**, 107002 (2005).

¹⁷M. B. Maple, P.-C. Ho, N. A. Frederick, V. S. Zapf, W. M. Yuhasz, E. D. Bauer, A. D. Christianson, and A. H. Lacerda, *J. Phys.: Condens. Matter* **15**, S2071 (2003).

¹⁸F. B. Anders, *Eur. Phys. J. B* **28**, 9 (2002).

¹⁹F. B. Anders, *Phys. Rev. B* **66**, 020504(R) (2002).

²⁰K. Miyake, H. Kohno, and H. Harima, *J. Phys.: Condens. Matter* **15**, L275 (2003).

²¹K. Maki, S. Haas, D. Parker, H. Won, K. Izawa, and Y. Matsuda, *Europhys. Lett.* **68**, 720 (2004).

²²Y. Aoki, T. Namiki, S. Ohsaki, S. R. Saha, H. Sugawara, and H. Sato, *J. Phys. Soc. Jpn.* **71**, 2098 (2002).

²³R. Vollmer, A. Faisst, C. Pfeleiderer, H. v. Lohneysen, E. D. Bauer, P.-C. Ho, V. Zapf, and M. B. Maple, *Phys. Rev. Lett.* **90**, 057001 (2003).

²⁴T. Tayama, T. Sakakibara, H. Sugawara, Y. Aoki, and H. Sato, *J. Phys. Soc. Jpn.* **72**, 1516 (2003).

²⁵P.-C. Ho, N. A. Frederick, V. S. Zapf, E. D. Bauer, T. D. Do, M. B. Maple, A. D. Christianson, and A. H. Lacerda, *Phys. Rev. B* **67**, 180508(R) (2003).

²⁶N. Oeschler, P. Gegenwart, F. Weickert, I. Zerec, P. Thalmeier, F. Steglich, E. D. Bauer, N. A. Frederick, and M. B. Maple, *Phys. Rev. B* **69**, 235108 (2004).

²⁷D. M. Broun, P. J. Turner, G. K. Mullins, D. E. Sheehy, X. G. Zheng, S. K. Kim, N. A. Frederick, M. B. Maple, W. N. Hardy, and D. A. Bonn, cond-mat/0310613 (unpublished).

²⁸E. E. M. Chia, M. B. Salamon, H. Sugawara, and H. Sato, *Phys. Rev. Lett.* **91**, 247003 (2003).

²⁹J. A. Sauls, *Adv. Phys.* **43**, 11 (1994).

³⁰R. Heffner and M. Norman, *Comments Condens. Matter Phys.*

- 17**, 361 (1996).
- ³¹K. Izawa, Y. Nakajima, J. Goryo, Y. Matsuda, S. Osaki, H. Sugawara, H. Sato, P. Thalmeier, and K. Maki, *Phys. Rev. Lett.* **90**, 117001 (2003).
- ³²M. Ichioka, N. Nakai, and K. Machida, *J. Phys. Soc. Jpn.* **72**, 11322 (2003).
- ³³D. E. MacLaughlin, J. E. Sonier, R. H. Heffner, O. O. Bernal, B.-L. Young, M. S. Rose, G. D. Morris, E. D. Bauer, T. D. Do, and M. B. Maple, *Phys. Rev. Lett.* **89**, 157001 (2002).
- ³⁴H. Kotegawa, M. Yogi, Y. Imamura, Y. Kawasaki, G.-q. Zheng, Y. Kitaoka, S. Ohsaki, H. Sugawara, Y. Aoki, and H. Sato, *Phys. Rev. Lett.* **90**, 027001 (2003).
- ³⁵Y. Aoki, A. Tsuchiya, T. Kanayama, S. R. Saha, H. Sugawara, H. Sato, W. Higemoto, A. Koda, K. Ohishi, K. Nishiyama, and R. Kadono, *Phys. Rev. Lett.* **91**, 067003 (2003).
- ³⁶K. Takegahara, H. Harima, and A. Yanase, *J. Phys. Soc. Jpn.* **70**, 1190 (2001).
- ³⁷E. A. Goremychkin, R. Osborn, E. D. Bauer, M. B. Maple, N. A. Frederick, W. M. Yuhasz, F. M. Woodward, and J. W. Lynn, *Phys. Rev. Lett.* **93**, 157003 (2004).
- ³⁸K. Kuwahara, K. Iwasa, M. Kohgi, K. Kaneko, S. Araki, N. Metoki, H. Sugawara, Y. Aoki, and H. Sato, *J. Phys. Soc. Jpn.* **73**, 1438 (2004).
- ³⁹R. Shina, M. Mastsumoto, and M. Koga, *J. Phys. Soc. Jpn.* **73**, 3253 (2004).
- ⁴⁰R. Shina and Y. Aoki, *J. Phys. Soc. Jpn.* **73**, 541 (2004).
- ⁴¹T. Goto, Y. Nemoto, K. Sakai, T. Yamaguchi, M. Akatsu, T. Yanagisawa, H. Hazama, K. Onuki, H. Sugawara, and H. Sato, *Phys. Rev. B* **69**, 180511(R) (2004).
- ⁴²P. Morin and D. Schmitt, *Phys. Rev. B* **23**, 5936 (1981).
- ⁴³K. Tenya, N. Oeschler, P. Gegenwart, F. Steglich, N. A. Frederick, E. D. Bauer, and M. B. Maple, *Acta Phys. Pol. B* **34**, 995 (2003).
- ⁴⁴S. Raymond, J. Flouquet, K. Kuwahara, K. Iwasa, M. Kohgi, K. Kaneko, N. Metoki, H. Sugarawa, Y. Aoki, and H. Sato, *Physica B* (to be published).
- ⁴⁵P. Nozières and A. Blandin, *J. Phys. (France)* **41**, 193 (1980).
- ⁴⁶A. Schiller, F. B. Anders, and D. L. Cox, *Phys. Rev. Lett.* **81**, 3235 (1998).
- ⁴⁷F. B. Anders, Habilitation thesis, Tech. Hochschule Darmstadt, 2001.
- ⁴⁸D. L. Cox and A. Zawadowski, *Adv. Phys.* **47**, 599 (1998).